ORIGINAL CONTRIBUTION

Microfluidic fabrication of polymer blend particles containing poly(4-butyltriphenylamine)-*block*-poly(methyl methacrylate): effect of block copolymer and rate of solvent evaporation on morphology

Ryoka Shoji[1] · Saki Yoshida[1] · Shu Kikuchi[1] · Shinji Kanehashi[1] · Kazuo Okamoto[2] · Guanghui Ma[3] · Kenji Ogino[1]

Abstract

Here, we reported particles with approximately 80-μm diameter with phase-separated morphology of ternary polymer blends containing poly(4-butyltriphenylamine) (PBTPA), poly(methyl methacrylate) (PMMA), and PBTPA-*b*-PMMA fabricated via a microfluidic emulsification technique with a Y-shaped microreactor followed by a solvent evaporation. Addition of block copolymer changed the macroscopic structure from core-shell to Janus and more complicated sea-island type with the increase of the block copolymer content. The Janus structure with a PMMA hemisphere containing small PBTPA domain was observed at 10 wt% of the block copolymer. Meanwhile, the rapid evaporation changed the morphology macroscopically from the Janus to the undeveloped one where PMMA-rich phase mainly located at center sandwiched with outside PBTPA phases, suggesting that morphologies are governed by the kinetical factors together with the conventionally accepted thermodynamic ones. After the solvent annealing with toluene, distinct and enlarged PMMA phase appeared radiately, of which size gradiently decreased from the surface to the center (200–500 nm) in each particle.

Keywords Janus · Block copolymer · Polymer blend · Polymer particle · Phase separation · Microreactor

Introduction

Recently, particles of polymer composites including polymer-polymer blends and hybrids with inorganic materials exhibiting various functionalities have been applied to biomedical fields [1], electric devices [2], and so on. The unique shapes and/or specific multi-phased morphologies have been sometimes observed affording the novel or improved functionalities [3–6] in polymer blend and hybrid particles resulted

✉ Shinji Kanehashi
  kanehasi@cc.tuat.ac.jp

✉ Kenji Ogino
  kogino@cc.tuat.ac.jp

1 Graduate School of Bio-Applications and Systems Engineering, Tokyo University of Agriculture and Technology, 2-24-16 Nakacho, Koganei-shi, Tokyo 184-8588, Japan

2 Ushio Chemix Co., Ltd., Kakegawa-shi, Shizuoka 437-1302, Japan

3 State Key Laboratory of Biochemical Engineering, Institute of Process Engineering, Chinese Academy of Sciences, Beijing 100080, People's Republic of China

from incompatibility of both polymers blends and aggregation of inorganic ingredients, respectively.

In previous works, a variety of seeded polymerizations have been utilized to control the inner morphologies such as Janus and core-shell structure [7–9]. As the other alternative, a solvent evaporation method, in which polymer particles are formed by the evaporation of the solvent from polymer solution droplets dispersed in an aqueous solution containing a surfactant, has been reported as a practical way to fabricate polymer particles. Since in situ polymerization process is not required, this method is applicable to various polymers including non-vinyl condensation polymers and polymers with a special structure like block copolymer [10–13]. For example, micron-sized particles with onion-like multilayered structure derived from block copolymers were fabricated by utilizing this method with the combination with a membrane emulsification method producing droplets of polymer solutions [14, 15]. In addition, much attention has been paid to microfluidic technique for the production of droplets, since it can afford uniform droplets and particles with over 100-μm diameters [16, 17].

Our research group previously reported the microfluidic approach to fabricate microspheres with a variety of morphologies based on the phase separated poly(4-butyltriphenylamine)

(PBTPA)/poly(methyl methacrylate) (PMMA) binary blends, where the combination of the microfluidic emulsification with a Y-shaped microreactor and the subsequent solvent evaporation method was utilized. According to this paper, final morphologies strongly depended on the initial conditions of dispersion including the droplet size and the concentration of polymer solutions, and it was suggested that the morphologies are governed by the kinetic factors together with the conventionally accepted thermodynamic ones [18]. Although PBTPA has been utilized as hole transporting materials [19, 20], it is also a promising material in optical application because of high refractive index of 1.71 at 633 nm and transparency in the visible light region. For example, by the combination with a polymer with relatively lower refractive index like PMMA, a refractive index modulation with large contrast is expected, which could be an important building block in optical applications [19–21].

Herein, we report the microfluidic fabrication of monodispersed particles with a diameter of 70–80 μm consisting of PBTPA/PBTPA-*b*-PMMA/PMMA ternary blends. The effects of the content of the block copolymer, solvent evaporation rate, and solvent annealing on the phase separated structure were investigated. The formation mechanism is also discussed based on the thermodynamic factors and the mobility difference for each component. To the best of our knowledge, few approaches have been reported on macro-sized particles with the diameter over 50 μm based on block copolymers. As a special case in larger size of blend particles, it is reported that a hierarchical structure resulted from dynamics, and manipulation of interface by the block copolymer was observed.

Experimental section

Materials

PBTPA and PMMA were synthesized by palladium-catalyzed C-N coupling and atom transfer radical polymerization (ATRP), respectively [22]. PBTPA-*b*-PMMA was prepared by Suzuki-Miyaura coupling of bromo-terminated PBTPA with PMMA modified with boronic ester at the end (see Supplementary Materials). The number average molecular weight (M_n) and polydispersity indices (PDI) were determined by gel permeation chromatography (GPC) calibrated with polystyrene standards, and the results are summarized in Table 1. Polymers were dissolved in chlorobenzene (Wako Pure Chemical Industries, Osaka, Japan) to have concentration of 1.0 *w/v*% for total polymers, and the resulting solution was used as a dispersed phase in an oil-in-water (O/W) emulsion. Poly(vinyl alcohol) (PVA) (PVA224, Kuraray, Tokyo, Japan) was used as a water-soluble stabilizer.

Fabrication of polymer blend particles

To produce microspheres of binary or trinary blend, O/W emulsion droplets were prepared using Y-shaped microreactor (YMC, Kyoto, Japan) [18]. The Y-channel for generating emulsions in the stainless steel mixer (30 mm×30 mm, 1.3 mm in thickness) is 0.5 mm wide and 0.1 mm deep. The dispersed and continuous phases were delivered from two gastight Hamilton syringes (Hamilton Company, Reno, NV, USA) with Lure-Lock fitting mounted syringe pumps onto the microreactor. The flow rates of the dispersed phase (polymer solution) and the continuous phase (aqueous 0.6 wt% of PVA solution) were fixed to 7 and 140 μL/min, respectively. The concentration of dispersed phase was adjusted to 1.0 *w/v*%. The weight ratio of PBTPA to PMMA was kept constant at 1:1. The droplets were collected in a three-necked 300-mL flask equipped with a mechanical stirrer without plugs containing 200 mL of the same aqueous solution as the continuous phase over 2 h at room temperature. The resulting dispersion was gently agitated with a mechanical stirrer at 70 rpm to evaporate chlorobenzene. The rate of solvent evaporation was controlled as follows. On the case of "slow (standard)" evaporation, the two mouths on the side necks (19 mm ID) of the three-necked flask were sealed with plugs. The evaporation without both plugs was regarded as "rapid" one. Completion of solvent evaporation was determined by observing the droplets every 24 h with an optical microscope. The produced microspheres were washed with distilled water four times with a centrifugation process.

Solvent annealing

The solvent annealing was carried out according to the literature [23]. Toluene (1.0 g) was emulsified in 10 g of a methanol/water (1/2, *w/w*) mixture containing 0.1% of sodium dodecyl sulfate (SDS) with an ultrasonic homogenizer at 0°C for 10 min. The resulting toluene emulsion was mixed with particle dispersion (particles/toluene 1/10, *w/w*), and the mixture was stirred with a mechanical stirrer at 70 rpm at room temperature for 24 h to allow the absorption of toluene and subsequently the evaporation of toluene.

Observation of polymer blend particles

To evaluate the morphologies of resulting particles, the observations with scanning electron microscope (SEM, JSM-6510, JEOL, Tokyo, Japan) and transmission electron microscope (TEM, JEM1400, JEOL, Tokyo, Japan) were carried out. In some cases, microspheres were washed with acetone to selectively remove PMMA phase to clarify the component in the phase-separated domain from SEM image since only PMMA is soluble in acetone. Specimens for SEM were prepared by putting one drop of methanol dispersion of the particles on the

Table 1 Molecular weight of PBTPA, PMMA, and PBTPA-*b*-PMMA

Polymer	M_n (PBTPA)/g mol^{-1}	M_n (PMMA)/g mol^{-1}	PDI	f_{PBTPA} [a]
PBTPA	4100		1.1	
PMMA		5500	1.5	
PBTPA-*b*-PMMA	8000[b]	9000[b]	1.8	0.49

[a] The volume fraction of PBTPA

[b] Determined by ^{1}H NMR

sample stage, and then dried in air. The samples were coated by gold (Au) using ion coater (IB-3, EIKO Engineering Co., Ltd., Japan) to avoid charging. To prepare the specimens for TEM observation, microspheres were embedded in a commercially available epoxy resin (a mixture of Quetol-812, dodecenyl succinic anhydride, methyl nadic anhydride, and DMP-30), and the thermosetted resin was processed into thin slices with 70 nm of thickness. To stain the PBTPA domain, the specimens were exposed to the vapor of an aqueous RuO$_4$ solution (0.5%) for 30 min in a sealed bottle at room temperature. From SEM images, the value of coefficient of variation (CV) was estimated by measuring the diameters of 100 particles.

Results and discussion

Effect of block copolymer content

Table 2 shows the results of the average diameter and coefficient of variation (CV) of the prepared particles. Figures 1 and 2 show the SEM and TEM images of ultrathin cross sections of the stained with RuO$_4$ vapor for 30 min, respectively. Uniform spherical particles were obtained regardless of the content of the block copolymer.

As previously reported [18], PBTPA/PMMA (50/50 *w/w*) blend particles showed core-shell morphology (PMMA; shell, and PBTPA; core, assigned from SEM images) (Fig. 1 a and b). Addition of 10 wt% of the block copolymer (PBTPA/PBTPA-*b*-PMMA/PMMA; 45/10/45 *w/w/w*%) altered the morphology to Janus type as shown in Fig. 1 c and d. Each morphology was confirmed by the SEM images for samples after soaking in

acetone, which can only dissolve PMMA domains. In Fig. 1 b and d, shrunken full spheres and hemispheres were observed, respectivey. In observed Janus particles, hemispheres composed of PMMA-rich phase contained PBTPA domains with a few micrometer size (Fig. 2b and Fig. S2 in Supplementary Materials), and PBTPA-rich hemispheres no PMMA domains (Fig. S3). These results suggest that block copolymer decreased the interfacial tension between the PBTPA-rich domain and the PVA aqueous solution.

With 50 wt% of the block copolymer (25/50/25 *w/w/w*%), no Janus particles were obtained, which was confirmed by SEM observation. As shown in Fig. 1f, distinct shapes like sphere and hemisphere were no longer observed after soaking in acetone. In fact, the particle was partially dissolved in acetone. It is considered that the observed collapsed shape after soaking was due to the complicated structure built up in the particles as shown in Fig. 2 d and e. At lower magnification (Fig. 2d), we can see the structure composed of micrometer-sized PMMA spherical domains and matrix consising of both components. At higher magnification (Fig. 2e), it is found that small PBTPA domains (tens of nanometer size) were coagulated in a PMMA matrix. That is why the original spherical shape was collapsed by soaking with acetone. It is noteworthy that soaked particles of block copolymer alone were larger than the original ones. Judging from SEM images of the surfaces (Fig. 1 g and h), soaked particles seem porous resulting from foaming during releasing of acetone. The increasing of the size is probably ascribed to this porous nature. As expected, the block copolymer alone afforded spherical particles with irregulary microphase-separated structure (Fig. 2 g and h).

Judging from obtained morphologies, it is considered that the addition of the block copolymer suppresses the

Table 2 Conditions and diameters of resulting polymer blend particles

| Conc. of block copolymer/ wt%	Average diameter/ μm	CV/ %	Days for solvent evaporation/ days	Morphology
0	83.1	10.9	8	Core-shell
10	84.1	11.8	8	Janus
50	71.2	13.6	5	Sea-islands
100	72.0	12.9	5	Disorder

CV coefficient of variation
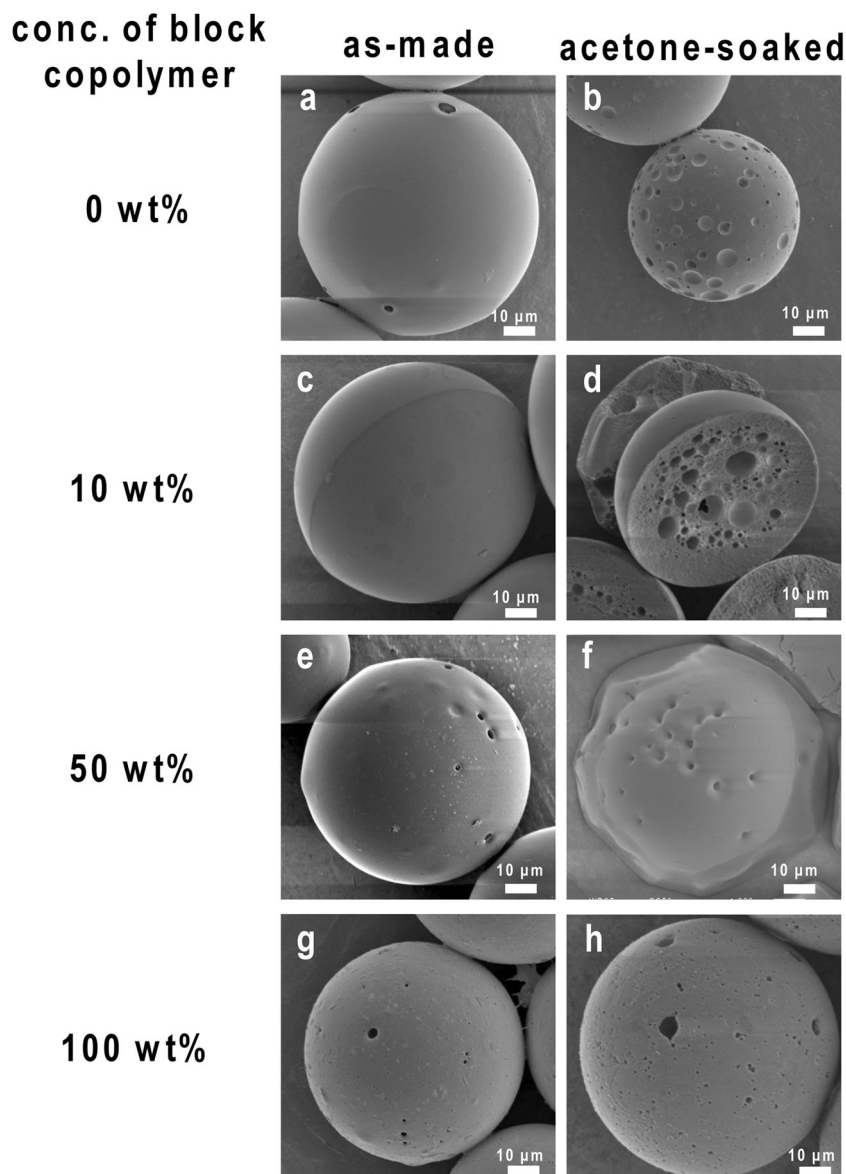
aggregations of PBTPA component in PMMA-rich phase. Figure 3 shows the plausible illustration of the effect of addition of the block copolymer in the formation of morphologies in the composite microsphere. In a previous paper, it has been demonstrated that the liquid-liquid phase separation of PBTPA-rich phase starts at the early stage of solvent evaporation due to the difference of solvation ability in the PBTPA/PMMA/chlorobenzene system to form the droplets [18]. In other words, at the initial stage, it is considered that the PBTPA-rich domains are dispersed in PMMA-rich domain (Fig. 3 a and f). After the further solvent evaporation, PBTPA-rich domains get denser accompanied with the exclusion of PMMA component and the coalescence to reach the final morphology. As illustrated in Fig. 3 b and g, the block copolymer locates predominantly at the interface of both phases and stabilizes the PBTPA-rich domain. Because of

the low degree of stabilization in the case of 10 wt% block copolymer, coalescence proceeds to form the large domains (Fig. 3c). Since block copolymer chains still locate at the interfaces, the difference of surface tensions to PVA solution between both domains seems smaller compared with the case of homopolymer blends, and resulting larger domain migrates to form the Janus structure. Since the solvent evaporation makes the PBTPA-rich domains less mobile, some portions of small spherical domains are left behind in PMMA-rich domain.
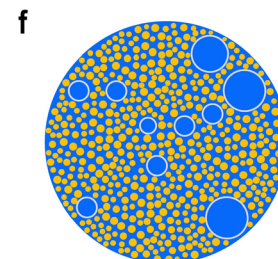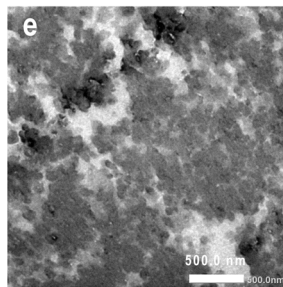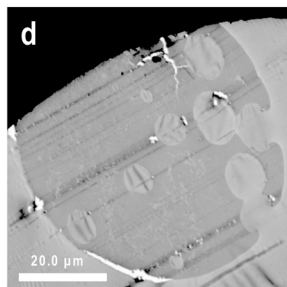
In the case of 50 wt% block copolymer, the aggregation of PBTPA-rich domains leads to larger domains, and the migration over long distance was limited, because of higher stabilization. In the local regions, however, the aggregation of PBTPA-rich domains occurred to some extent. Even after solidification of PBTPA
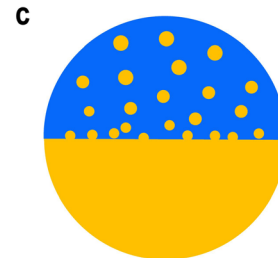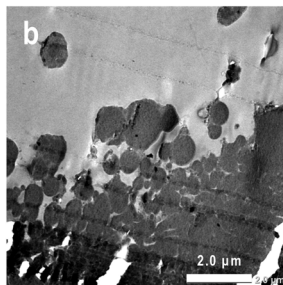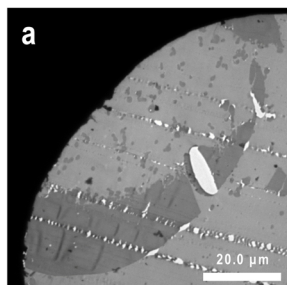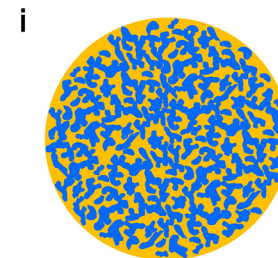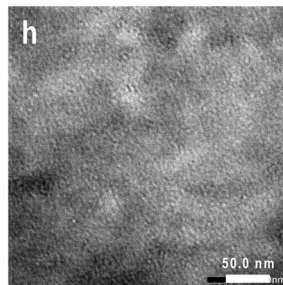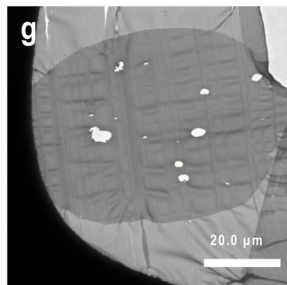
Fig. 2 TEM photographs of PBTPA/PBTPA-*b*-PMMA/PMMA blend particles and schematic representation for observed morphologies [PBTPA/PBTPA-*b*-PMMA/PMMA (*w/w/w*): **a**, **b**, **c** 45/10/45; **d**, **e**, **f** 25/50/25; **g**, **h**, **i** 0/100/0]. TEM images at low (**a**, **d**, **g**) and high (**b**, **e**, **h**) magnification; schematic models (**c**, **f**, **i**), blue: PMMA, orange: PBTPA

phase, more mobile PMMA-rich phase assembled accompanied with the exclusion of PBTPA-rich domain to form thermodynamically stable sphere domains (Fig. 3 i and j).

Effect of rate of solvent evaporation

For the PBTPA/PBTPA-*b*-PMMA/PMMA (45/10/45 *w/w/w*) blend, we fabricated the particles prepared with different rates
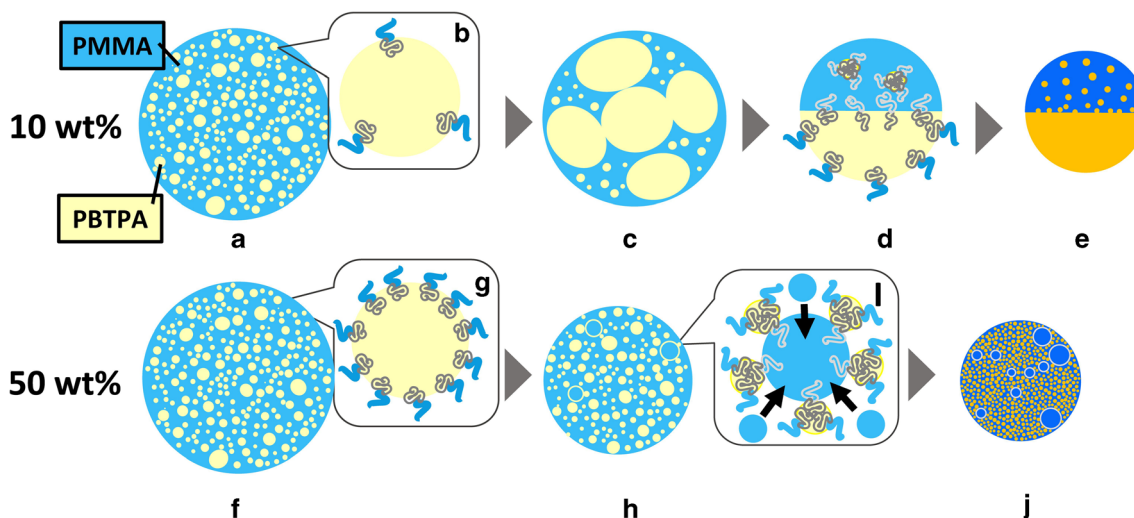

Fig. 3 Plausible illustration of the effect of addition of PBTPA-*b*-PMMA in the formation of PBTPA/PMMA composite microsphere (sky blue: PMMA-rich solution, pale yellow: PBTPA-rich solution, blue: PMMA-rich domain, orange: PBTPA-rich domain)

of the solvent evaporation and observed the structural changes. On the conditions in Figs. 1 and 2, the evaporation process was carried out using a three-necked flask with plugs, in which it took 8 days to evaporate the solvent almost completely, and the Janus morphology was observed. On the other hand, without plugs, only 2 days was necessary. From SEM images of resulting particles in Fig. 4, the particles with undeveloped phase separated structure (at least 4 types) were obtained. In addition, as shown in Fig. 5, it is confirmed that PBTPA phases located outside the particles. Furthermore, it is found that PBTPA-rich spherical domains with tens of nanometer were dispersed in the PMMA-rich domain.

Assuming that thermodynamically stable structure is Janus type for PBTPA/PBTPA-b-PMMA/PMMA (45/10/45 w/w/w) blend, it is reasonable that small PBTPA-rich domains produced at the early stage coalesce and migrate to approach Janus structure (Fig. 6a–c). The final structure is determined by the interfacial tension between PVA aqueous solution and each component. The rapid evaporation leads to the steady concentration gradient inside the droplets, the phase separation, and subsequent coalescence proceeds earlier near the surface than around the center (Fig. 6e). Earlier solidification of the larger domains near the surface prohibits the long distance migration. In the case of the rapid evaporation, it is considered that the additional dynamical limitation brought about the undeveloped structure. Therefore, it is considered that some portions of small spherical domains were left behind in PMMA-rich domain due to low mobility of PBTPA-rich domains. Consequently, the morphology at the earlier stage was frozen in this region.

Effect of annealing with toluene

SEM and TEM photographs of PBTPA/PBTPA-b-PMMA/ PMMA (45/10/45 w/w/w) blend particles fabricated with rapid evaporation after the annealing with toluene are shown in Fig. 7. In the SEM photographs (Fig. 7a, b), the macroscopic structual change was not obseved. In the TEM photographs, in the PMMA-rich phase, spherical PMMA domains with 1 μm or less were formed radially from the interface with the PBTPA-rich domain toward the center of the particle (Fig. 7d). In addition, the domains near the interface were larger than those around the center of particle. Magnified TEM images before and after annealing are shown in Fig. 8. As shown in Fig. 8 a and b, the distinct and smooth interface was observed before annealing, and irregular one was observed after annealing. These observations suggest that the migration of small PBTPA-rich domains over the interface is to be coalesced with large ones.

Figure 9 illustrates the plausible mechanism for the morphology change after annealing with toluene. Judging from results in Figs. 7 and 8, it is found that annealing level was not so high as to change the macroscopic structure. This means that the absorbed toluene distributed with the concentration gradient in a radial direction as shown in Fig. 9 b and c and mainly existed near the surface corresponding to the region between two broken lines (Fig. 9b). In PMMA-rich domain especially near the surface designated by the sky-blue-colored region in Fig. 9 d and e, the absorbed toluene made the frozen PBTPA small domains more mobile resulting in the migration of swollen PBTPA small domains designated by the pale yellow-colored region to PBTPA-rich domains as

Fig. 4 SEM photographs and schematic models of particles fabricated with rapid solvent evaporation (blue: PMMA, orange: PBTPA)
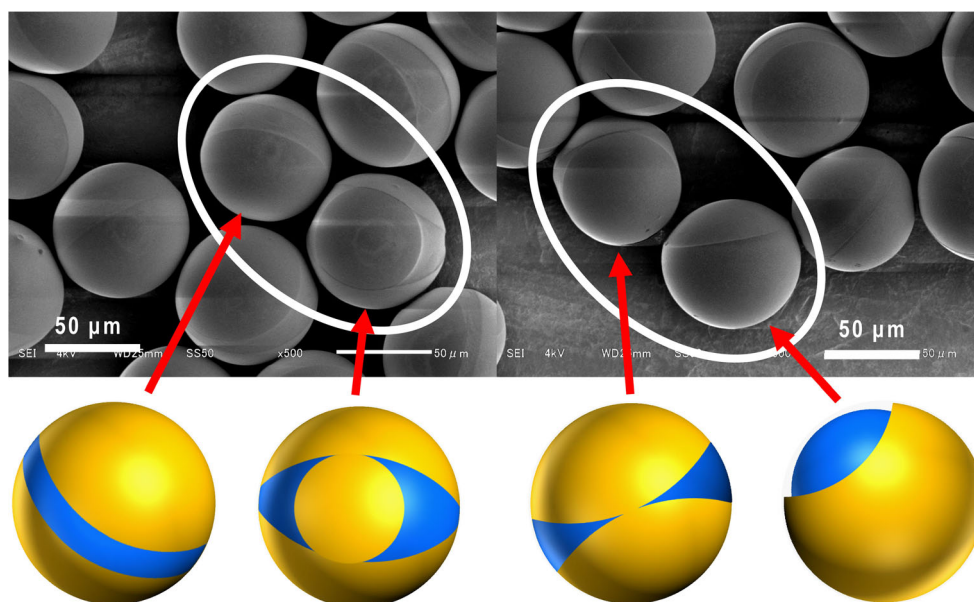
Fig. 5 TEM photographs (**a**, **c**) of particles shown in Fig. 4, and schematic models, (**b**, **d**) for **a** and **c**, respectively (blue: PMMA-rich, orange: PBTPA-rich). TEM photographs at high magnification of interface of both domains, (**e**) and PMMA-rich domain (**f**)
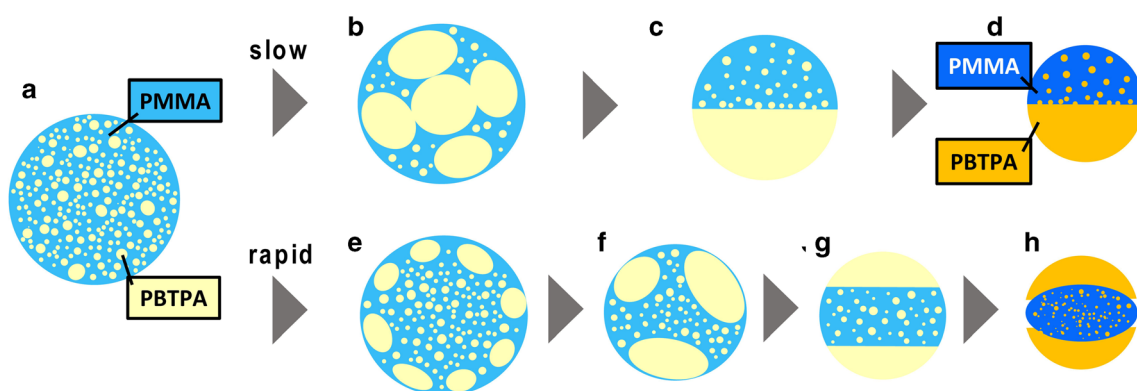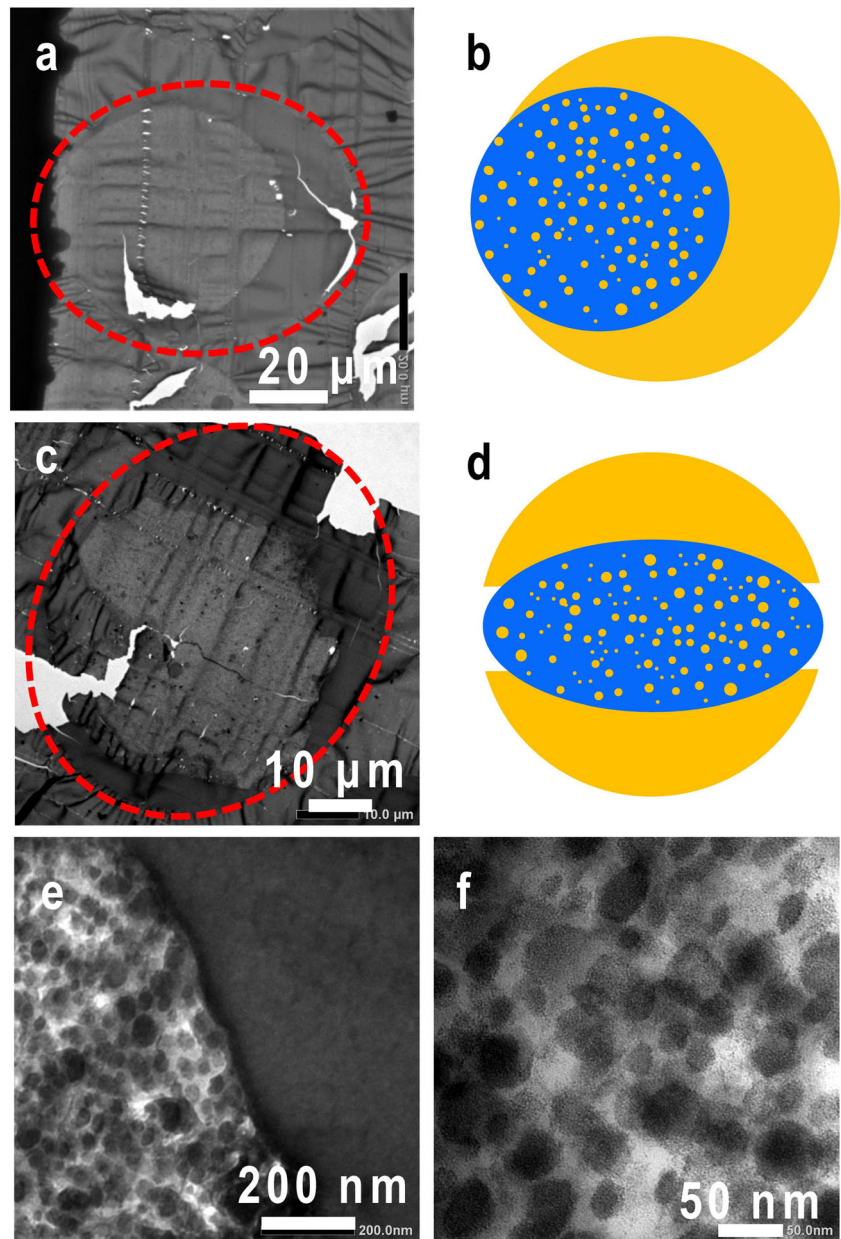

Fig. 6 Schematic illustration of the effect of rate of solvent evaporation (sky blue: PMMA-rich solution, pale yellow: PBTPA-rich solution, blue: PMMA-rich domain, orange: PBTPA-rich domain)
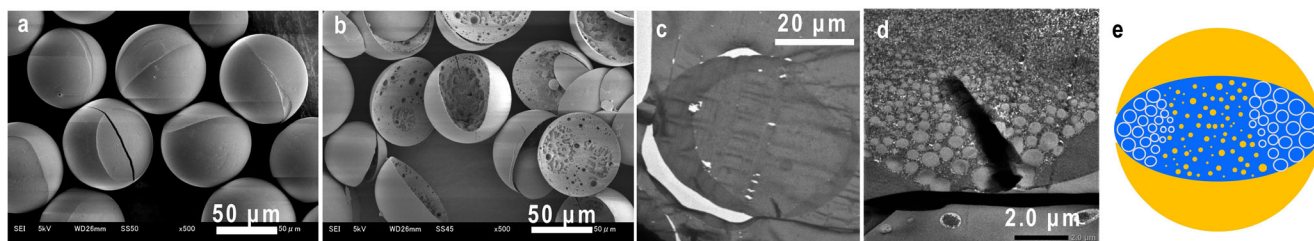
Fig. 7 Microscopic images of particles after annealing. SEM image before (**a**) and after, (**b**) washing with acetone; TEM images at low, (**c**) and high, (**d**) magnification; schematic model* as shown in **e**. Blue: PMMA-rich, orange: PBTPA-rich. *The schematic model was determined by TEM photographs (Fig. 7d and Figure S4 in Supplementary Materials)

shown in Fig. 9d. Simultaneously, PBTPA domains dispersed in more mobile PMMA domains were excluded, and decontaminated PMMA domains assembled to form thermo-dynamically stable sphere domains as shown in Fig. 9e. As a result, the hierarchical structure was formed inside the particle (Fig. 9f).
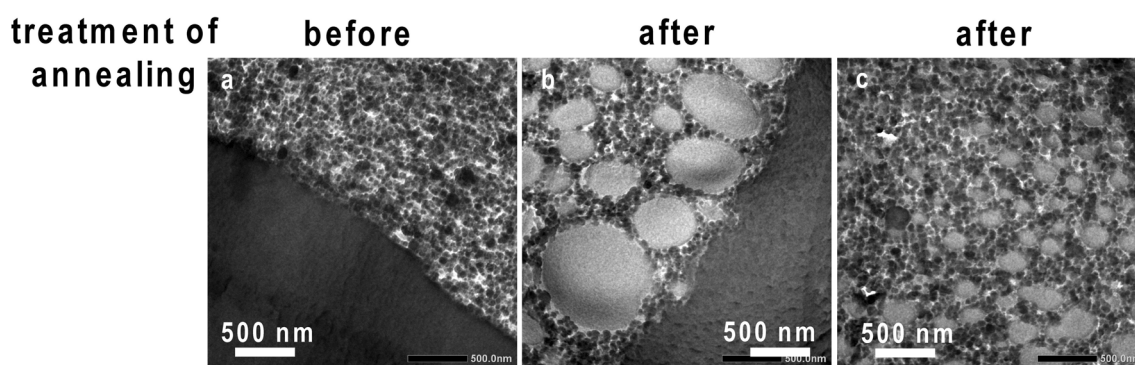

Fig. 8 TEM photographs of before and after annealing. **a** Interface with PBTPA and PMMA, **b** interface with PBTPA and PMMA, **c** center of the particle
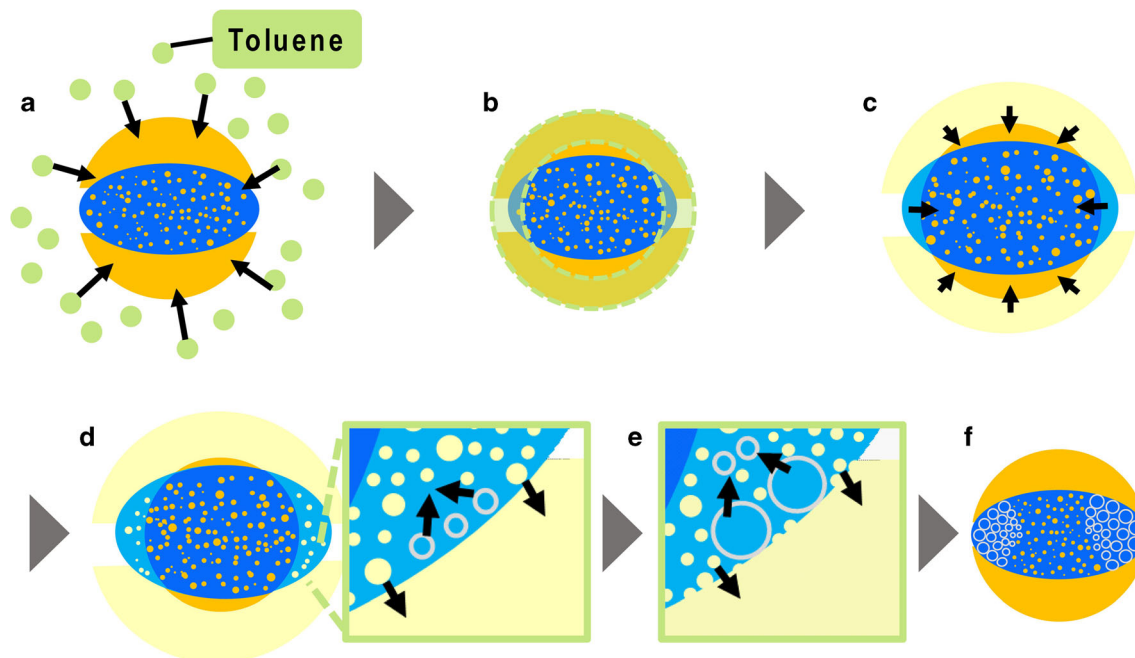

Fig. 9 Illustration of morphology change after annealing with toluene (sky blue: swollen PMMA, pale yellow: swollen PBTPA, blue: PMMA, orange: PBTPA)

Conclusion

We reported here the fabrication of uniform-sized microspheres consisting of ternary blend, PBTPA, PMMA, and PBTPA-*b*-PMMA with various phase-separated morphologies utilizing the combination of microfluidic emulsification with a Y-shaped microreactor and the solvent evaporation. Amount of block copolymer influenced domain size in a droplet. In the case of 10 wt% of block copolymer, microspheres with Janus type structure were formed although the core-shell morphology was observed without the block copolymer. In the particles consisting of 50 wt% of block copolymer, more complicated sea-island morphology was observed. These can be explained by thermodynamical modification of interface by addition of block copolymer and the kinetic limitation. In the rapid evaporation, the structure turned from Janus type to the specific one in which PBTPA phases located outside. This structure could be explained by the temporary concentration gradient inside the droplets resulted from the rapid evaporation. Although solvent anealing with toluene changed no macroscopic morphology, one micron or less-sized spherical PMMA domains appeared and its size increased radially from the center. The formation of the phase-separated structure inside the microspheres can be explained both from thermodynamical and kinetic points of view. It is suggested that our approach can be applied to the fabrication of microspheres with the index modulation in the range from nano to micron size. If the size regularly lies in sub-micron range, the single microsphere manipulates the visible light in optical applications.

Supplementary Information The online version contains supplementary material available at https://doi.org/10.1007/s00396-021-04817-6.

Declarations

Conflict of interest The authors declare that they have no conflict of interest.

References

1. Mora-Huertas CE, Fessi H, Elaissari A (2010) Polymer-based nanocapsules for drug delivery. Int J Pharm 385:113–142. https://doi.org/10.1016/j.ijpharm.2009.10.018
2. Nisisako T, Torii T, Takahashi T, Takizawa Y (2006) Synthesis of monodisperse bicolored Janus particles with electrical anisotropy using a microfluidic co-flow system. Adv Mater 18:1152–1156. https://doi.org/10.1002/adma.200502431
3. Tu F, Lee D (2012) Controlling the stability and size of double-emulsion-templated poly(lactic-*co*-glycolic) acid microcapsules. Langmuir 28:9944–9952. https://doi.org/10.1021/la301498f
4. Charreyre MT, Boullanger P, Delair T, Pichot C (1993) Preparation and characterization of polystyrene latexes bearing disaccharide surface groups. Colloid Polym Sci 271:668–679. https://doi.org/10.1007/BF00652829
5. Urakami Y, Kasuya Y, Fujimoto K, Miyamoto M, Kawaguchi H (1994) Phagocytosis of microspheres with modified surfaces. Colloids Surf B 3:183–190. https://doi.org/10.1016/0927-7765(94)80065-0
6. Kawamura A, Michinari K, Morimoto G, Nannichi Y, Taniguchi T, Kishikawa K (2016) Full-color biomimetic photonic materials with iridescent and non-iridescent structural colors. Sci Rep 633984. https://doi.org/10.1038/srep33984
7. Okubo M, Izumi J, Takekoh R (1999) Production of micron-sized monodispersed core/shell composite polymer particles by seeded dispersion polymerization. Colloid Polym Sci 277:875–880. https://doi.org/10.1007/s003960050464
8. Li B, Wang M, Chen K, Chang Z, Chen G, Zhan Z (2015) Synthesis of biofunctional Janus particles. Macromol Rapid Commun 36:1200–1204. https://doi.org/10.1002/marc.201500063
9. Skelhon TS, Chen Y, Bon SAF (2014) Synthesis of "hard–soft" Janus particles by seeded dispersion polymerization. Langmuir 30:13525–13532. https://doi.org/10.1021/la503366h
10. Ospina-Villa JD, Gomez-Hoyos C, Zuluaga-Gellego R, Trina-Chavez O (2019) Encapsulation of proteins from Leishmania panamensis into PLGA particles by a single emulsion-solvent evaporation method. J Microbiol Methods 162:1–7. https://doi.org/10.1016/j.mimet.2019.05.004
11. Kimura S, Hyodo T, Shimizu Y, Egashira M (2008) Preparation and characterization of polyethylene-based hybrid particles by an environmentally-friendly and aqueous solvent evaporation method. Colloids Surf A Physicochem Eng Asp 318:206–216. https://doi.org/10.1016/j.colsurfa.2007.12.035
12. Ito F, Fujimori H, Honnami H, Kawakami H, Kanamura K, Makino K (2009) Study of types and mixture ratio of organic solvent used to dissolve polymers for preparation of drug-containing PLGA microspheres. Eur Polym J 45:658–667. https://doi.org/10.1016/j.eurpolymj.2008.12.037
13. Shin JM, Kim Y, Yun H, Gi-Ra Y, Kim J (2017) Morphological evolution of block copolymer particles: effect of solvent evaporation rate on particle shape and morphology. ACS Nano 11:2133–2142. https://doi.org/10.1021/acsnano.6b08342
14. Tanaka T, Saito N, Okubo M (2009) Control of layer thickness of onionlike multilayered composite polymer particles prepared by the solvent evaporation method. Macromolecules 42:7423–7429. https://doi.org/10.1021/ma901100n
15. Higuchi T, Tajima A, Yabu H, Shimomura M (2008) Spontaneous formation of polymer nanoparticles with inner micro-phase separation structures. Soft Matter 4:1302–1305. https://doi.org/10.1039/B800904J
16. Li W, Zhang L, Ge X, Xu B, Zhang W, Liangliang Q, Choi C-H, Xu BJ, Zhang A, Lee H, Weitz DA (2018) Microfluidic fabrication of microparticles for biomedical applications. Chem Soc Rev 47:5646–5683. https://doi.org/10.1039/C7CS00263G
17. Sharratt WN, Brooker A, Robles ESJ, Cabral JT (2018) Microfluidic solvent extraction of poly(vinyl alcohol) droplets: effect of polymer structure on particle and capsule formation. Soft Matter 14:4453–4463. https://doi.org/10.1039/C7SM02488F
18. Yoshida S, Kikuchi S, Kanehashi S, Okamoto K, Ogino K (2018) Microfluidic fabrication of morphology-controlled polymeric microspheres of blends of poly(4-butyltriphenylamine) and poly(methyl methacrylate). Materials 11:582. https://doi.org/10.3390/ma11040582
19. Cao Z, Abe Y, Nagahama T, Tsuchiya K, Ogino K (2013) Synthesis and characterization of polytriphenylamine based graft polymers for photorefractive application. Polymer 54:269–276. https://doi.org/10.1016/j.polymer.2012.11.028
20. Tsuchiya K, Kikuchi T, Songeun M, Shimomura T, Ogino K (2011) Synthesis of diblock copolymer consisting of poly(4-butyltriphenylamine) and morphological control in photovoltaic

application. Polymers 3:1051–1064. https://doi.org/10.3390/polym3031051

21. Kikuchi S, Yoshida S, Kanehashi S, Ma G-H, Ogino K (2019) Fabrication of core-shell, Janus, dumbbell, snowman-like and confetti-like structured microspheres of blends of poly (4-butyl triphenylamine) and poly (methyl methacrylate) by solvent evaporation method. J Fiber Sci Technol 75:022–028. https://doi.org/10.2115/fiberst.2019-0004

22. Kikuchi S, Kanehashi S, Ogino K (2018) Transition of phase-separated PBTPA/PMMA solution droplets from core–shell to Janus morphology under UV light irradiation. Polym J 50:1089–1092. https://doi.org/10.1038/s41428-018-0104-0

23. Okubo M, Takekoh R, Saito N (2004) Formation mechanism of an "onionlike" multilayered structure by reconstruction of the morphology of micron-sized, monodisperse poly(methyl methacrylate)/polystyrene composite particles with the solvent-absorbing/solvent-releasing method. Colloid Polym Sci 282:1192–1197. https://doi.org/10.1007/s00396-004-1057-8